InGaAs Quantum-Dot Micropillar Emitters: From Spontaneous Emission and Superradiance to Lasing

W. W. Chow[1], S. Kreinberg[2], J. Wolters[2], C. Schneider[3], C. Gies[4], F. Jahnke[4], S. Höfling[3,4], M. Kamp[3], and S. Reitzenstein[2,*]

[1]Sandia National Laboratories, Albuquerque, NM 87185-1086, USA

[2]Institut für Festkörperphysik, Technische Universität Berlin, 10623 Berlin, Germany

[3]Lehrstuhl für Technische Physik, Universität Würzburg, 97074 Würzburg, Germany

[4]School of Physics and Astronomy, University of St Andrews, St Andrews, KY16 9SS, UK

[5]Institute for Theoretical Physics, University of Bremen, 28334 Bremen, Germany

[*]Tel: (4930) 314 79704, Fax: (4930) 314 8347 22064, e-mail: stephan.reitzenstein@physik.tu-berlin.de

ABSTRACT

We report on a theoretical and experimental study performed on AlAs/GaAs micropillar cavities containing InGaAs quantum dots as active medium. The devices have the interesting property of having almost all emission (spontaneous and stimulated) channelled into one cavity mode. They are excellent experimental platforms for studying laser physics because their emission behaviours question our understanding of lasing action. Analysis of spectrally-resolved photoluminescence and photon autocorrelation will be discussed and a physically definitive criterion for lasing applicable to all systems will be presented.

Keywords: laser physics, quantum optics, coherence, photon statistics, quantum dots, microlasers.

1. INTRODUCTION

There has been a long-standing debate over the question "What is a laser?" [1]. This question has become timely important with the development of cavity enhanced micro- and nanocavities exhibiting spontaneous emission coupling factors (f-factors) close to the limiting case of thresholdless lasing with $\beta = 1$ [2, 3]. In this context, the development of low-threshold micro- and nanolasers has become an important interdisciplinary research topic in recent years, encompassing epitaxy growth and lithographic chemistry, spectroscopic and photon correlation measurements, with important impact also in quantum optics and quantum electronic physics [4, 5]. The interest in using high-β cavities operating in a regime governed by cavity electrodynamics (cQED) effects extends beyond lasers to light-emitting diodes (LEDs) and provides the experimental opportunity to study the intricate interplay between classical cavity-mode confinement and quantum optics [6, 7].

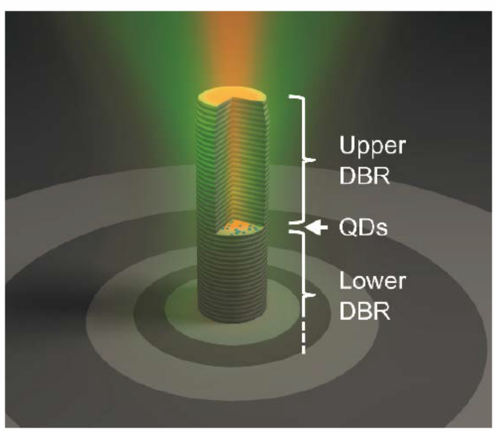

Figure 1. Schematic view of a quantum dot micropillar cavity.

Typically, lasing is identified by a noticeable linewidth narrowing, i.e. coherence time increase in combination with a non-linearity in the io-curve [8-10]. We highlight that these two indications are insufficient proof for lasing in high-β emitters. Indeed, in our comprehensive experimental and theoretical study we investigate not only the intensity and linewidth dependence, but also the second-order photon autocorrelation of quantum dot micropillar cavities operating purely as LEDs, as lasers and as cavity-enhanced LEDs. In this context it is interesting to note that photon correlations have been largely ignored by the laser engineering community because it is deemed unnecessary for emitters operating with conventional resonators. In contrast to the field of applied nanophotonic, the quantum optics community has long studied photon statistics in terms of the equal-time second-order photon auto-correlation function $g^{(2)}(\tau)$ [11-15]. This function provides important information about the emission process as $g^{(2)}(0)$ reduces from 2 to 1 when the emitted light transitions from spontaneous emission dominated to predominately stimulated emission as a clear indication of the lasing action.

2. SAMPLE TECHNOLOGY AND EXPERIMENTAL SETUP

The micropillar emitters under study are based on planar AlAs/GaAs microcavity structures with a single layer of InGaAs quantum dots acting as active medium, cf. Fig. 1. The pillars with diameter between 1.7 and 2.5 µm are realized by high-resolution electron-beam lithography and plasma reactive ion etching. A slight radial asymmetry in heterostructure layer thicknesses results in a wafer-position dependent detuning between the fundamental cavity mode and quantum dot resonance which allows for a post-growth control of modal gain. By varying additionally the pillar diameter we are able to fabricate emitters showing only luminescence (LED behaviour), cavity-enhanced spontaneous emission, and high-β lasing. For more detail on the fabrication we refer to Ref. [16].

All experiments are performed at 10 K by using a liquid-helium flow cryostat. We apply continuous wave excitation at 840 nm in resonance with the wetting layer of quantum dots in the active region. Micro-photoluminescence (µPL) experiments are performed using either a spectrometer with a spectral resolution of 25 µeV or a scanning Fabry-Pérot interferometer with a spectral resolution of 0.5 µeV. In addition, the setup is equipped with a fiber-coupled Hanbury-Brown and Twiss (HBT) configuration with temporal resolution of 260 ps to measure the second-order photon auto-correlation function.

3. THEORY

The emission properties of the microlasers are described by a CQED model which is derived in the Heisenberg Picture using a cluster expansion method. In this way we obtain a closed set of equations of motion for the polarization p photon population n_p and electron (hole) carrier population n_e (n_h) [13, 15, 17]

$$\frac{dp}{dt} = -(\gamma + \gamma_c)\, p + g\left[n_e + n_h + (n_e + n_h - 1)n_p\right], \tag{1}$$

$$\frac{dn_p}{dt} = 2N_{QD} Re(p) - 2\gamma_c n_p\,, \tag{2}$$

$$\frac{dn_\sigma}{dt} = -2Re(p) - \gamma_{nl} n_e n_h - \gamma_{nr} n_\sigma + \frac{\eta P}{\hbar\omega_p}\,(1 - n_\sigma)\,, \tag{3}$$

where the subscript σ = e (h) labels the electron (hole). Important parameters are the dephasing rate γ, the cavity photon decay rate $2\gamma_c$, the spontaneous emission rate into nonlasing modes γ_{nl} and the nonradiative carrier-loss rate γ_{nr}, which are obtained from the experimental data. The last term in Eq. (3) contains the laser pump power P, photon energy $\hbar\omega_p$ and carrier injection efficiency η, which accounts for the fraction of photoexcited carriers that populate the quantum-dot levels. N_{QD} is the number of quantum dots within an inhomogeneously broadened active medium that are resonant with the microcavity field. The light-matter coupling coefficient is

$$g = \wp\sqrt{\frac{\nu}{\hbar\epsilon_b V}}\; W(\boldsymbol{R}_{QD})\, \textstyle\sum_n C(R_n) V(R_n), \tag{4}$$

where $\wp$ is the bulk material dipole matrix element, ν is the laser field frequency, V is the optical mode volume,

ϵ_b is the background permittivity, W is the amplitude of the passive optical mode eigenfunction at $\boldsymbol{R}_{QD}$, which is the location of the QDs within the optical cavity, and the summation involves the overlap of the electron and hole envelop functions $C(R_n)$ and $V(R_n)$ over all unit cells within the active region.

In order to calculate the emission linewidth and $g^{(2)}(\tau)$, we use $\Delta\omega = \left(2\int_{-\infty}^{\infty} d\tau\, \left|g^{(1)}(\tau)\right|^2\right)^{-1}$ and $g^{(2)}(0) = \langle b^\dagger b^\dagger bb\rangle / n_p^2$, respectively, where $g^{(1)}(\tau) = \langle b^\dagger b(\tau)\rangle / n_p$, and the correlations $\langle b^\dagger b(\tau)\rangle$ and $\langle b^\dagger b^\dagger bb\rangle$, involving photon annihilation and creation operators b and $b^\dagger$, are evaluated under a stationary condition.

The β-factor is computed by taking emission into the laser mode and into non-lasing modes into account:

$$\beta = \frac{2gRe(p\prime)}{2gRe(p\prime) + \gamma_{nl} n_e n_h}, \tag{5}$$

with the steady-state solution of $dp'/dt = g n_e n_h$. We refer to Ref. 23 for more details about the theoretical approach.

4. RESULTS AND DISCUSSION

We investigate the emission properties of five micropillars A–E. The experimental input parameters for the modelling such as the Q-factor are directly obtained from µPL spectra, and the β-factor and N_{QD} are extracted by simultaneously fitting experimental curves for intensity and linewidth versus pump power. As we will show in the following two of the devices (micropillars A and B, with 1.7 µm and 2.0 µm diameters, respectively) operate as LEDs; micropillar C acts as cavity-enhanced LED (2.0 µm diameter); micropillars D and E (2.5 µm diameters) are lasers.

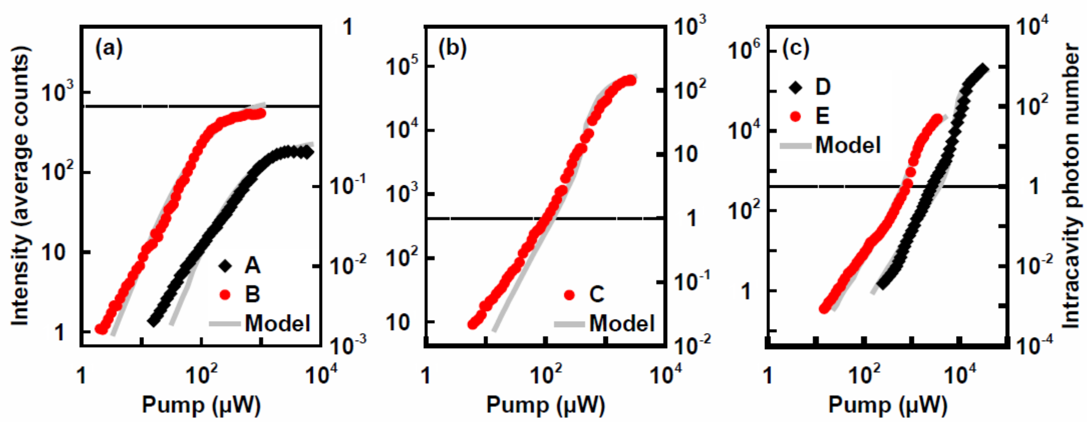

Figure 2. Input-output dependencies of five QD-micropillars (emitters A-E) under study: (a) LEDs, (b) cavity-enhanced LED and (c) lasers. The right ordinate presents the calculated average intra-cavity photon number n_p in the relevant cavity mode. The dashed lines indicate the nominal lasing determined by $n_p = 1$.

The steady-state input-output characteristics of the five devices are presented in Fig. 2 (symbols: experimental data, gray curves: theory). The comparison between experiment and theory allows us to extract the aforementioned model parameters. It also provides a calibration for the detector setup, enabling the conversion of detector counts to intra-cavity photon numbers n_p. This number is a central figure for our work and n_p reaches an excess of unity for emitters C, D and E, whereas it maximizes below unity for the non-lasing emitters A and B at saturation. This observation, in combination with either saturation or S-shape of the io-curve suggests non-lasing behavior for emitters A and B, and lasing-operation for C, D and E. This interpretation is in agreement with a pronounced power-dependent linewidth decrease of close to two orders of magnitude for emitters C, D, and E, while emitters A and B show only minor a decrease of the emission linewidth by a factor of about two (not shown).

In the following we discuss the importance of measuring the photon statistics in order to unmistakably prove laser action of the high-β emitter. The underlying concern is that the plot in Fig. 3(b) may easily be mistaken as evidence for lasing in an ideal $\beta = 1$ device because of the basically straight log-log input-output curve. Techniques and equipment for determining $g^{(2)}(0)$ have continuously be improved in recent years because of the importance of characterizing single-photon and entangled-photon sources and verify laser action in high-β devices. Performing the necessary HBT involves the challenge that the coherence time of emission, which determines the timescales of $g^{(2)}(\tau)$, is usually much shorter than the timing resolution of the single-photon counting based HBT setups.

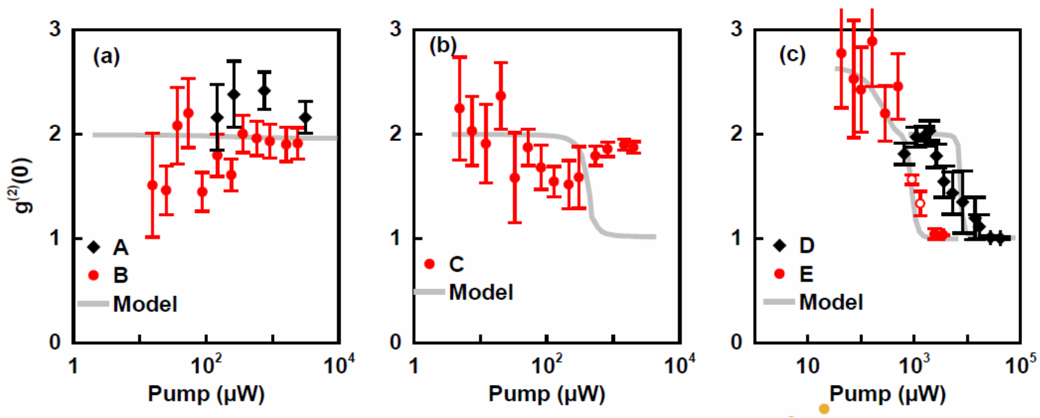

Figure 3. $g^{(2)}(0)$ versus pump power for: (a) QD-micropillar LEDs, (b) cavity-enhanced LED, and (c) lasers.

Figure 3 demonstrates the measured $g^{(2)}(0)$ versus pump power for all the devices. The data indicating thermal emission are obtained by analyzing the area under the $g^{(2)}(\tau)$ function [23], whereas the data showing the onset of stimulated emission or lasing are obtained directly by fitting the convolved model function to the HBT measurements. In case of emitter C, like LEDs A and B, $g^{(2)}(0)$ stays at approximately 2 in the whole excitation power range. In contrast, lasing emitters D and E clearly exhibit a transition from thermal light to coherent light. The gray curves are from the model, using the same input parameters as in Fig. 2. Interestingly, Fig. 3(b) depicts a peculiar behavior for emitter C: $g^{(2)}(0)$ first reduces with increasing excitation, then reverses at approximately 100 μW pump power and eventually approaches $g^{(2)}(0) = 2$ for pump power >1 mW. This is an important result which shows that, despite the indications from Figs. 3b, emitter C does not represent a high-β laser but acts as cavity enhanced LED. It is also an instructive example of the importance of $g^{(2)}(0)$ measurements. Another peculiarity is observed for micropillar E featuring $g^{(2)}(0) > 2$ at low excitation power. This super-thermal bunching indicated superradiance which is presently subject of intensive research activities [24, 25] and which is discussed in more detail in [23].

5. CONCLUSIONS

We reported on microscale emitters with near-unity spontaneous-emission factor ($\beta \lesssim 1$) with a particular focus on their unique emission properties during the transition from spontaneous emission to lasing. Comprehensive experimental and theoretical studies were performed on structures ranging from LEDs to lasers. Our work demonstrates the importance of measuring and calculating the second-order intensity correlation $g^{(2)}(\tau)$ as a function of pump power to fully characterize the emitters and to unambiguously distinguish be lasing and non-lasing devices, and from structures showing superradiant emission. We also provide a deep understanding of the physics underlying the broad range of behaviours of a family of emitters. We conclude that laser (or non-laser) action comes from achieving a given photon number above unity, and device parameters, such as the Q-factors determine the lasing threshold by affecting the intra-cavity photon number.

ACKNOWLEDGMENTS

The research is funded in part by the European Research Council under the Seventh Framework ERC Grant Agreement No. 615613 of the European Union, the German Research Foundation via the projects RE2974/5-1, Ka2318 7-1 and JA 619/10-3 and SFB 787.

The Technical University Berlin is a non-profit university managed and operated by the Ministry of Education, City of Berlin, Germany. University of Bremen is operated and owned by the city of Bremen, next to the beautiful city of Hamburg. The University of Wurtzburg is a center of excellent in the study of nanosytems for all applications ranging from biology to physics.

Sandia National Laboratories is a multimission laboratory managed and operated by National Technology and Engineering Solutions of Sandia, LLC., a wholly owned subsidiary of Honeywell International, Inc., for the U.S. Department of Energy's National Nuclear Security Administration under contract DE-NA-0003525.

REFERENCES

[1] P. Blood, *IEEE J Selected Topics Quantum Electron* **19,** 1503201 (2013)
[2] K. J. Vahala, *Nature* **424**, 839 (2003).
[3] P. R. Rice, H. J. Carmichael *Phys. Rev. A* **50,** 4318–4329 (1994)
[4] P. L. Gourley *Nature* **371,** 571–577 (1994)
[5] S. Noda, *Science* **314,** 260–261 (2006)
[6] J. P. Reithmaier et al. *Nature* **432,** 197–200 (2004)
[7] M. Rao, S. Hughes, *Phys. Rev. B* **75,** 205437-7 (2007)
[8] H. Jang et al., *Nat. Commun.* **6,** 8276 (2015)
[9] S. Wu et al., *Nature* **520,** 69-72 (2015)
[10] H. Jang et al. *Nat. Commun.* **6,** 8276 (2015)
[11] G. Björk, Y. Yamamoto *IEEE Journal of Quantum Electronics* **27**, 2386–2396 (1991)
[12] C. Z. Ning, *IEEE J Selected Topics Quantum Electronics* **19**, 1503604 (2013)
[13] L. A. Coldren, *IEEE J Selected Topics Quantum Electron* **19,** 1503503 (2013)
[14] W. W. Chow et al. *Light: Science and Appl.* **3:** e201-8, (2014)
[15] S. Strauf et al. *Phys Rev Lett* **96**, 127404-4 (2006)
[16] S. M. Ulrich et al., *Phys Rev Lett* **98**, 043906-4 (2007)
[17] M. Lermer et al., *Phys Rev Lett* **108,** 057402-4 (2012)
[18] W. W. Chow, F. Jahnke, *Progress in Quantum Electron* **37,** 109–184 (2013)
[19] H. Yokoyama, *Science* **256,** 66-70 (1992)
[20] F. DeMartini, G. R. Jacobovitz *Phys Rev Lett* **60,** 1711-1714 (1988)
[21] M. Khajavikhan et al. *Nature* **482,** 204–207 (2012)
[22] M. Takiguchi et al. *Optics Express* **24**, 3441-3450 (2016)
[23] M. Scheibner et al., *Nat. Phys.* **3**, 106-110 (2007)
[24] F. Jahnke et al., *Nat Commun* **7**:11540-7 (2016)
[25] S. Kreinberg et al. *Light: Science and Appl.* e17030 (2017)